Acta Oncologica, 2006; 45: 915–922

Taylor & Francis
Taylor & Francis Group

ORIGINAL ARTICLE

Respiration correlated cone-beam computed tomography and 4DCT for evaluating target motion in Stereotactic Lung Radiation Therapy

THOMAS G. PURDIE[1,2], DOUGLAS J. MOSELEY[1,2], JEAN-PIERRE BISSONNETTE[1,2], MICHAEL B. SHARPE[1,2], KEVIN FRANKS[3], ANDREA BEZJAK[2,3] & DAVID A. JAFFRAY [1,2]

[1]*Department of Radiation Physics, Princess Margaret Hospital/Ontario Cancer Institute, Toronto, Ontario, Canada,* [2]*Department of Radiation Oncology, University of Toronto, Toronto, Ontario, Canada and* [3]*Department of Radiation Oncology, Princess Margaret Hospital, Toronto, Ontario, Canada.*

Abstract

An image-guidance process for using cone-beam computed tomography (CBCT) for stereotactic body radiation therapy (SBRT) of peripheral lung lesions is presented. Respiration correlated CBCT on the treatment unit and four dimensional computed tomography (4DCT) from planning are evaluated for assessing respiration-induced target motion during planning and treatment fractions. Image-guided SBRT was performed for 12 patients (13 lesions) with inoperable early stage non-small cell lung carcinoma. Kilovoltage (kV) projections were acquired over a 360 degree gantry rotation and sorted based on the pixel value of an image-based aperture located at the air-tissue interface of the diaphragm. The sorted projections were reconstructed to provide volumetric respiration correlated CBCT image datasets at different phases of the respiratory cycle. The 4D volumetric datasets were directly compared with 4DCT datasets acquired at the time of planning. For ten of 12 patients treated, the lung tumour motion, as measured by respiration correlated CBCT on the treatment unit, was consistent with the tumour motion measured by 4DCT at the time of planning. However, in two patients, maximum discrepancies observed were 6 and 10 mm in the anterior-posterior and superior-inferior directions, respectively. Respiration correlated CBCT acquired on the treatment unit allows target motion to be assessed for each treatment fraction, allows target localization based on different phases on the breathing cycle, and provides the facility for adaptive margin design in radiation therapy of lung malignancies. The current study has shown that the relative motion and position of the tumour at the time of treatment may not match that of the planning 4DCT scan. Therefore, application of breathing motion data acquired at simulation for tracking or gating radiation therapy may not be suitable for all patients — even those receiving short course treatment techniques such as SBRT.

Stereotactic body radiation therapy (SBRT) has gained considerable interest as technological advancements in in-room imaging and body immobilization have improved target localization accuracy. The hallmarks of SBRT include prescription to doses with high biological effectiveness, inhomogeneous dose distributions within the target volume and hypo-fractionated treatment schedules. Such demands allow little room for target localization errors that are often unrecoverable in this context. Target localization is further complicated by both intra and inter-fraction target respiratory motion. Therefore, treatment margins are added to provide adequate target dose coverage with consideration for rapid dose falloff to limit normal tissue toxicity.

The clinical data for the treatment of early stage non-small cell lung cancer (NSCLC) using SBRT is limited. However, SBRT clinical studies using image-guidance and stereotactic immobilization for target localization, have demonstrated local control rates $>80\%$ with limited normal tissue toxicity [1–6], which are potentially comparable to surgical resection. By contrast, the local control rate is between 30–60% for medically inoperable patients undergoing conventional radiation therapy. Sibley et al. [7] showed in a series of stage I NSCLC patients undergoing conventional radiation therapy that 42% of failures occurred locally and 35% of deaths were attributed to cancer progression. These failures, occurring in the treatment field, suggest insufficient

Correspondence: T. G. Purdie, Princess Margaret Hospital, University Health Network, 610 University Avenue (5-814), Toronto, Ontario, CANADA M5G 2M9. Tel: +416 946 4501 x5814. Fax: +416 946 6566. E-mail: Tom.Purdie@rmp.uhn.on.ca

(Received 5 July 2006; accepted 11 July 2006)

ISSN 0284-186X print/ISSN 1651-226X online
DOI: 10.1080/02841860600907345

radiation dose and inaccurate targeting may be responsible for the discrepancy between surgical resection and conventional radiation therapy results.

SBRT techniques that deliver high biologically effective doses using accurate target localization via image-guidance or stereotactic immobilization, may limit failures within the treatment field. However, tumour motion due to respiration must still be addressed. In particular, a moving target necessitates larger treatment margins, which ultimately limit the dose to the target in order to achieve acceptable normal tissue toxicity. Tumour motion also confounds target delineation on volumetric images, adding to the uncertainty in treatment planning and delivery and increasing the likelihood of geographic miss.

The image-guidance system presented in the current study allows both target localization and tumour motion monitoring. Similarly, Uematsu et al. [2,4,8] have previously reported on image-guidance systems developed for SBRT, which incorporate a conventional linear accelerator, computed tomography (CT) scanner and x-ray simulator in the treatment room. The CT scanner provides excellent soft-tissue imaging for target localization and the simulator allows tumour motion monitoring. The same investigators developed a CT on rails system, in which the CT gantry moves instead of the couch when scanning, thereby reducing the potential for patient motion between imaging and treatment [9]. Following this work, Onishi et al. [10] developed a CT on rails image-guidance system to assess tumour position with a switching mechanism to synchronize the duration of irradiation with self-breath-holding without respiratory monitoring devices.

In the current study, the image-guidance process for SBRT of early stage NSCLC at Princess Margaret Hospital is presented. As with other image-guided approaches, the images of the target itself are used for localization. The ability to acquire in-room volumetric images precludes the need for frame-based stereotactic fiducials (Stereotactic Body Frame (SBF), Elekta Oncology Systems, Crawley, UK), thereby eliminating potential biases and offsets introduced from using external surrogates [11]. In this regard, kV cone-beam computed tomography (CBCT) imaging has been employed to generate 3-D volumetric datasets at the time of treatment [12]. In addition, the paper demonstrates the feasibility of incorporating respiration correlated CBCT into the image-guided process. Respiration correlated CBCT allows tumour motion to be assessed at the time of treatment [13–15], allows target localization based on multiple phases of the breathing cycle and facilitates on-line adaptive treatment planning by providing image datasets to verify or set treatment margins for each fraction.

Methods

Patients

Twelve patients with early stage NSCLC treated using a stereotactic image-guided approach and 4DCT have been analyzed for the purposes of this study. All patients were consecutively planned and treated on an Institutional Research Ethics Board approved protocol of SBRT for medically inoperable stage I/II NSCLC.

Target volumes

Treatment planning was conducted using the Pinnacle^3 treatment planning system (Philips Radiation Oncology Systems, Milpitas, CA). In seven patients, the target was delineated on a helical CT with contrast media. The gross tumour volume (GTV) was expanded by an asymmetric margin to generate a planning target volume (PTV) according to the Radiation Therapy Oncology Group Phase II clinical trial on hypofractionated stereoactic lung radiation therapy (RTOG 0236). In five patients, the target was delineated on the maximum inspiration and maximum expiration CT datasets from 4DCT respiratory sorting. These two datasets were fused to generate the internal target volume (ITV) as defined by IRCU Report 62 [16]. The ITV represents the target volume accounting for internal organ motion. A uniform 0.5 cm margin was added to the ITV to generate a PTV that explicitly includes both respiratory motion of the target and set-up uncertainty.

Immobilization and abdominal compression

Patients were immobilized using the SBF and vacuum pillow conforming to the patient external contour. The stereotactic fiducials embedded in the SBF for target localization were removed, as fiducials were not necessary for target localization. Moreover, the fiducials generated artefacts in the CBCT volumes and portal images. In four patients, the abdominal compression feature of the SBF was employed to limit target motion as determined at fluoroscopy prior to CT simulation.

CT simulation and 4DCT

CT simulation was performed using either a LightSpeed QXi 4-slice CT scanner or a Discovery hybrid PET/CT 16-slice scanner (GE Medical Systems,

Waukesha, WI). Patient respiration was monitored using an external marker (Real-time Position Management or RPM, Varian Medical Systems, Palo Alto, CA) system. A small block with reflective markers was placed on the patient's thorax and an infrared video camera mounted to the CT couch recorded the displacement of the block. The RPM system acquired the position of the block to continually measure the breathing cycle throughout the cine scan. Such breathing traces are used, in turn, to retrospectively correlate cine CT images with breathing phase [17]. The average breathing time was between 3–6 s and the time between cine images was 0.3–0.4 s to collect ten phases in the respiratory cycle. Figure 1 shows the 4DCT planning images for a patient with an upper lobe lung lesion at maximum inspiration and maximum expiration phases.

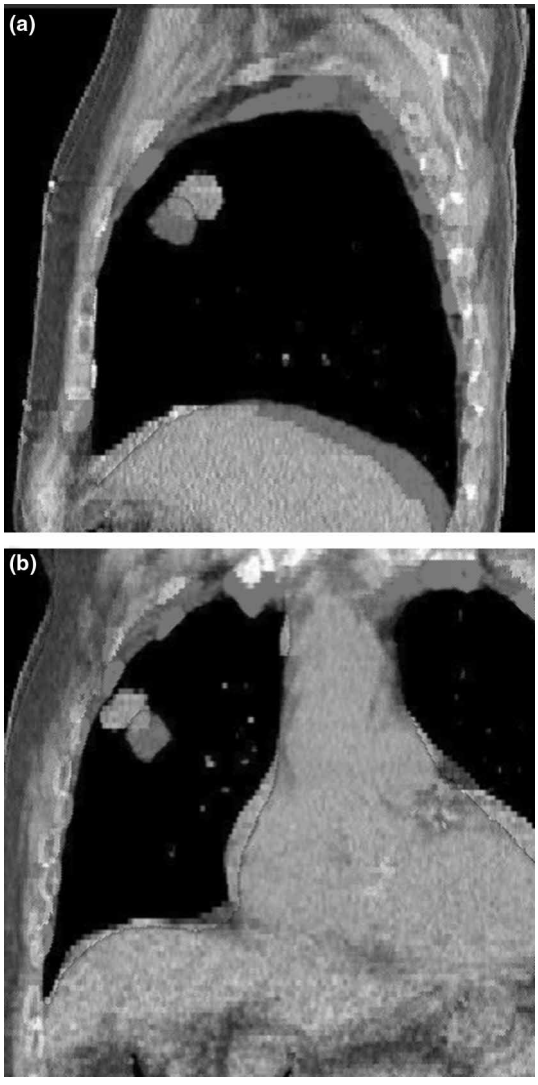

Figure 1. 4DCT planning images at maximum inspiration and expiration phases for a patient with an upper lobe lung lesion in (a) sagittal and (b) coronal orientations.

Treatment planning

Non-coplanar and non-opposing static 6 megavoltage (MV) x-ray beams were used to deliver inhomogeneous dose distributions within the PTV. Higher doses were produced at the centre of the target with sharp dose falloff at the periphery of the PTV. The multi-leaf collimator (MLC) was primarily conformed to the PTV, although a limited number of segmented beams were used to improve dosimetric coverage of larger lesions. Treatment fractions were separated by 2–7 day intervals and treatment courses were 8–13 days.

Image-guidance

Treatment delivery and in-room image-guidance were performed on a linear accelerator with kV imaging capabilities (Synergy, Elekta Oncology Systems, Crawley, UK). Sharpe et al. [18] have described the Synergy unit at Princess Margaret Hospital and Jaffray et al. [12] have previously detailed a similar unit. Briefly, the Synergy system is comprised of a kV x-ray tube and an amorphous silicon flat panel detector mounted directly onto to the gantry drum of the linear accelerator. In this way, the imaging and treatment planes are orthogonal to one another. The system was used to verify the position of the patient immediately prior to the delivery of radiation therapy. The daily CBCT datasets reconstructed from all projections were compared with the reference CT datasets from planning to establish the couch shift required to reposition the target at the accelerator isocentre.

Respiration correlated CBCT

Sonke et al. [14] have previously detailed a method for generating respiration correlated CBCT image datasets. Briefly, only x-ray projections that correspond to the same respiratory phase are reconstructed to generate multiple phase-based datasets. The volumetric datasets reconstructed in this way are less susceptible to motion artefacts and often provide better target delineation. We have developed a similar off-line methodology for phase determination directly from the x-ray projections used to reconstruct cone-beam CT volumetric datasets. This approach eliminates the need for tertiary surrogates (e.g. RPM) and reduces the potential for systematic phase offsets [13]. A 10 cm by 4 cm rectangular aperture (i.e. region of interest) is placed on the 2D projection image to encompass the air-tissue interface of the diaphragm as shown in Figure 2 (a). The mean pixel intensity is computed within this 2D aperture. During inspiration, more lung tissue fills the aperture on the projection image and

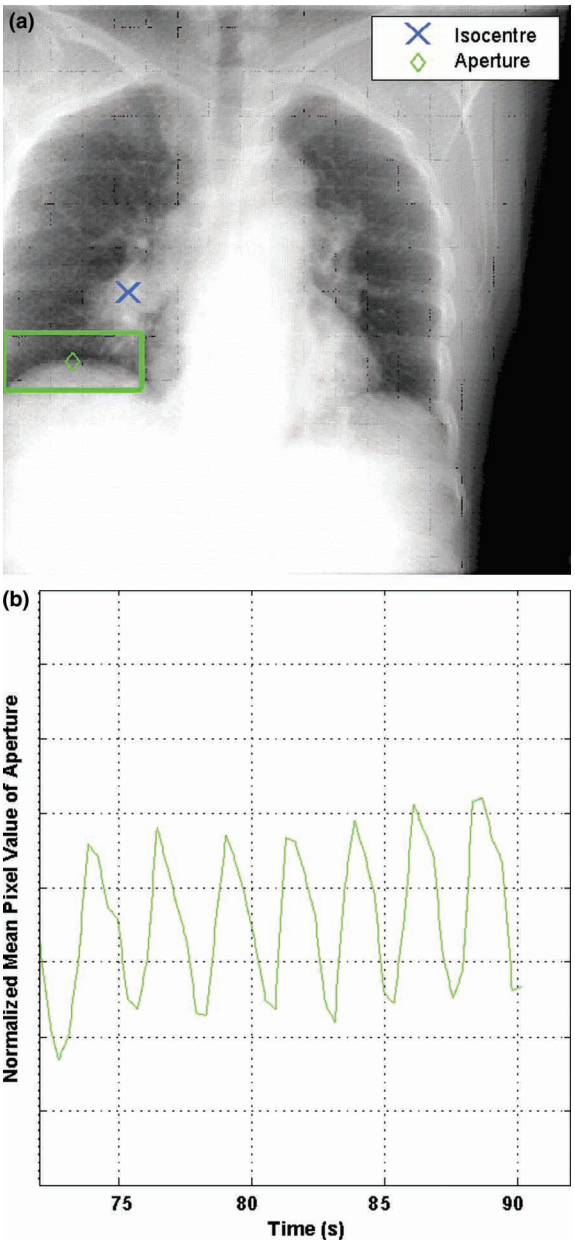

Figure 2. kV projection used for CBCT reconstruction is shown in (a). The diaphragm and lesion are clearly visible on the projection with the aperture at the air-tissue interface. A trace used for sorting kV projections is shown in (b). The normalized mean pixel value of the aperture is calculated for each projection.

the decreased attenuation will cause the mean pixel intensity to decrease as shown in Figure 2 (b). The opposite effect is seen during expiration. Hence, this signal increases and decreases with respiration and can be used to classify the respiration phase of each 2D projection. The projections are then binned based on a 10% amplitude threshold, to acquire the number of respiration phases desired. Each phase is reconstructed separately yielding a corresponding number of reconstructed volumetric image sets.

The gantry requires 4 minutes to rotate through 360 degrees, acquiring a total of approximately 640 projections. The inspiration and expiration datasets are typically reconstructed from approximately 130 and 160 projections, respectively. The imaging parameters, for the respiration correlated CBCT acquisition, are 120 kVp and 0.8 mAs per projection for an estimated imaging dose of approximately 0.02 Gy.

Respiration-correlated reconstructions of the expiration phase show a marked increase in lung detail and a reduction of diaphragm blurring artefacts. The variations in projection density over 360 degrees result in streak artefacts in the reconstruction at various phases. Tumour motion was determined retrospectively by measuring the amplitude of the target displacement between the maximum inspiration and maximum expiration phases. The same methodology was used to measure tumour motion from the 4DCT image datasets. All 3D displacements were performed in the treatment planning system.

Results

Figure 3 shows images for target localization for the patient in Figure 1. The CBCT image is matched to the planning CT image. The CBCT image datasets was reconstructed from the full projection set with a pixel pitch of 1 mm in all dimensions. From the full projection set, the projections at maximum inspiration and maximum expiration were used to generate respiration correlated CBCT images shown in Figure 4. The image datasets acquired using respiration correlated CBCT at the time of treatment can be used to compare to the 4DCT image data acquired at the time of planning, although both methods employ different surrogates and data for sorting.

Table I shows the volumes of the targets treated for each patient. In seven of the 12 patients, a helical scan was done to comply with the RTOG 0236 study; however a 4DCT scan was also acquired to assess target motion. Table I indicates the PTV volume based on both helical and 4DCT for these patients. For 11 patients treated, targets were peripheral and located in the upper lobe. In one patient, the lesion was in the lower lobe and adjacent to both the stomach and heart. For this patient, we used a more conservative dose fractionation schedule to limit normal tissue toxicity.

Table II shows the 4DCT measured tumour motion at the time of planning and the average tumour motion for each treatment fraction measured using respiration correlated CBCT at the treatment unit. The data represents the tumour amplitude in three dimensions following target localization using the full projection CBCT dataset and the reference CT dataset for matching. Four of

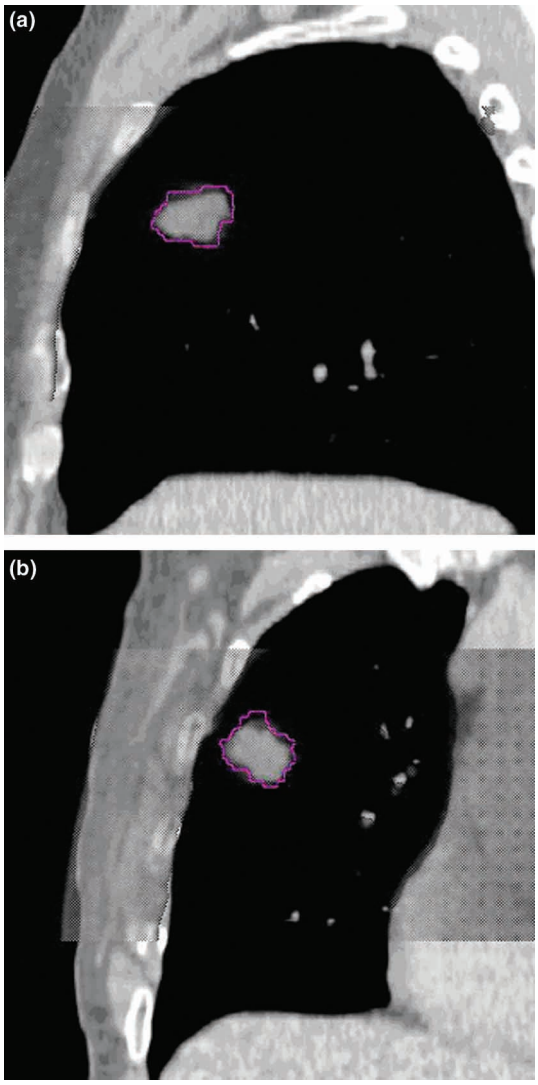

Figure 3. The matched planning CT and CBCT images used for target localization for one fraction. The GTV from planning is outlined. The CBCT images were reconstructed from the full projection set for the patient in Figure 1 in (a) sagittal and (b) coronal orientations.

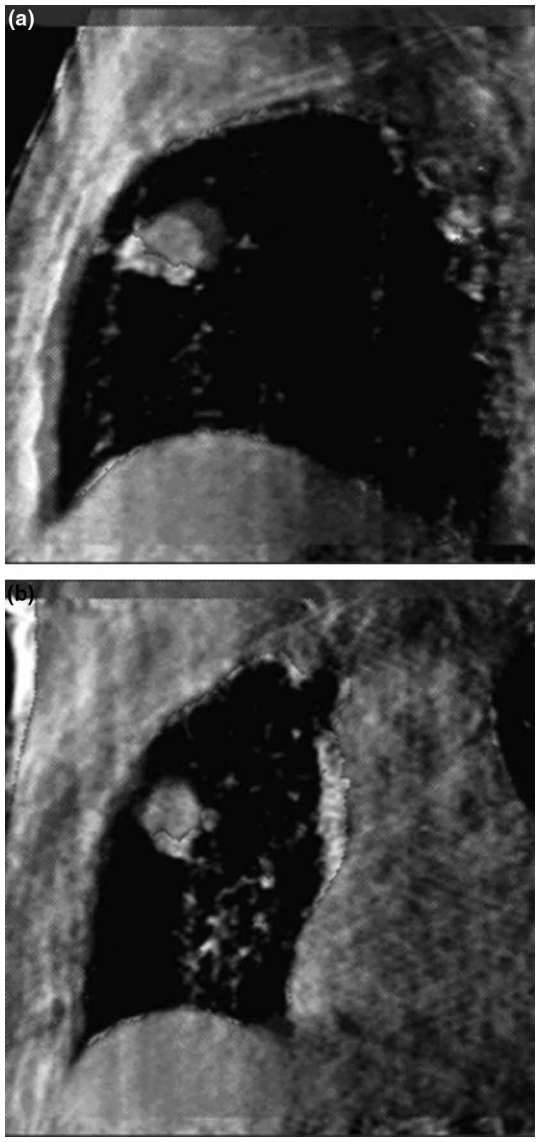

Figure 4. Respiration correlated CBCT images at maximum inspiration and maximum expiration for patient in Figures 1 and 3 in (a) sagittal and (b) coronal orientations.

the 12 patients treated had abdominal compression to limit tumour motion.

Figure 5 shows the difference in tumour motion between 4DCT and respiration correlated CBCT for each treatment fraction. The measured tumour motion is consistent across the population, with the exception of two patients. The maximum differences were 6 mm in the anterior-posterior direction and 10 mm in the superior-inferior direction, respectively.

Discussion

The importance of target localization in lung SBRT cannot be overstated. Moreover, target localization has to be addressed from both a spatial and temporal perspective. The image guidance approach presented here captures the volume, location and motion of the target, thereby providing information for target localization, validating fixed or patient-specific margins established at planning, and assessing the reproducibility of methods to limit tumour motion such as breath-hold and active breathing control (ABC).

The patients treated in this study are medically inoperable due to poor lung function or other significant co-morbidities. Therefore, breath-hold and ABC techniques, which are treatment options in the management of thoracic malignancies, may not be suitable for patients with limited lung capacity undergoing SBRT. Onishi et al. [10], using a CT on rails image-guidance system has shown excellent reproducibility in tumour position with patient

Table I. Target Volumes Measured from Planning CT.

Patient	GTV (cm^3)	PTV–Helical (cm^3)[1]	PTV–4DCT (cm^3)[2]	Tumour Location		
				LR	AP	SI
1 (L)	2.6	–	13.8	Left	Ant	Upper
1 (R)	14.7	–	53.0	Right	Centre	Mid
2	2.7	–	15.4	Left	Post	Upper
3	23.7	76.6	63.2	Right	Post	Mid
4	2.8	22.0	16.5	Right	Ant	Upper
5	7.1	32.7	39.5	Right	Ant	Upper
6	19.9	78.5	–	Left	Centre	Mid
7	11.8	–	40.7	Right	Post	Upper
8	5.1	–	21.5	Right	Centre	Upper
9	5.6	29.6	22.6	Left	Post	Upper
10	9.0	–	30.0	Left	Centre	Lower
11	10.0	40.1	30.9	Right	Post	Upper
12	0.9	10.7	8.3	Right	Centre	Upper

[1]PTV margin for helical CT: 0.5 cm LR, 0.5 cm AP and 1.0 cm SI according to RTOG 0236 protocol.
[2]PTV margin for 4DCT: 0.5 cm LR, 0.5 cm AP and 0.5 cm SI.

under self-breath-hold. Their results show tumour motion of 1.3 ± 0.5 mm in the left-right (LR) direction, 1.4 ± 0.6 mm in the anterior-posterior (AP) direction and 2.2 ± 1.1 mm in the superior-inferior (SI) direction.

Hoisak et al. [11] have demonstrated the relationship between external surrogate and tumour motion are not reproducible over multiple fractions and without daily concurrent imaging to directly measure tumour motion, the use of surrogates to guide radiation therapy may result in missing the target. From our experience, tumour motion at the time of treatment may not match the tumour motion from planning. In one patient, tumour motion measured by respiration correlated CBCT was greater than planning 4DCT by 9 mm and 10 mm, for two treatment fractions, respectively. The results presented here are similar to the findings by Underberg et al. [19]. In their study, either multiple helical scans or a single 4DCT scan was acquired to assess target motion at planning and throughout SBRT treatment on the CT simulator. In the current study, imaging data was acquired on the linear accelerator, prior to the start of treatment, and tumour motion was retrospectively measured. Their results showed no significant change in target motion between planning and over the course of treatment; however, there were substantial intra-patient changes between fractions, with the largest discrepancy between planning and treatment of 10 mm.

Table II. 4DCT and Respiration Correlated CBCT measured Tumour Motion.

Patient	Abdominal Compression Applied	Tumour Motion from 4DCT Planning Scan (mm)			Tumour Motion from Respiration Correlated CBCT (mm)[1]		
		LR	AP	SI	LR	AP	SI
1 (L)	No	0.1	1.7	0.4	0.5 ± 0.3	2.7 ± 1.0	1.3 ± 0.5
1 (R)	No	2.4	2.2	2.2	2.0 ± 0.3	2.1 ± 1.1	1.7 ± 0.4
2	No	0.7	1.0	3.1	0.5 ± 0.1	1.1 ± 1.2	3.0 ± 0.3
3	Yes	0.8	1.4	5.4	0.3 ± 0.1	0.9 ± 0.3	5.1 ± 2.7
4	No	1.2	3.3	1.4	1.0 ± 0.5	1.9 ± 1.4	1.4 ± 0.6
5	Yes	6.8	8.4	2.8	4.5 ± 0.5	3.9 ± 1.6	0.7 ± 0.1
6	No	–	–	–	3.8 ± 2.5	4.2 ± 1.2	3.4 ± 0.4
7	No	0.0	2.2	1.7	0.6 ± 0.2	0.5 ± 0.4	0.6 ± 0.6
8	No	0.3	0.2	1.1	0.3 ± 0.1	1.3 ± 0.6	1.3 ± 1.1
9	No	0.0	0.8	0.6	0.7 ± 0.5	2.5 ± 0.6	1.2 ± 0.9
10	Yes	0.6	2.9	6.4	3.2 ± 1.2	5.6 ± 2.6	12.2 ± 4.2
11	Yes	0.7	1.6	4.2	0.3 ± 0.3	1.1 ± 1.2	3.8 ± 0.2
12	No	0.1	1.4	2.1	0.8 ± 0.3	2.1 ± 1.2	3.2 ± 0.1

[1]Mean tumour motion for three fractions $\pm$ standard deviation.

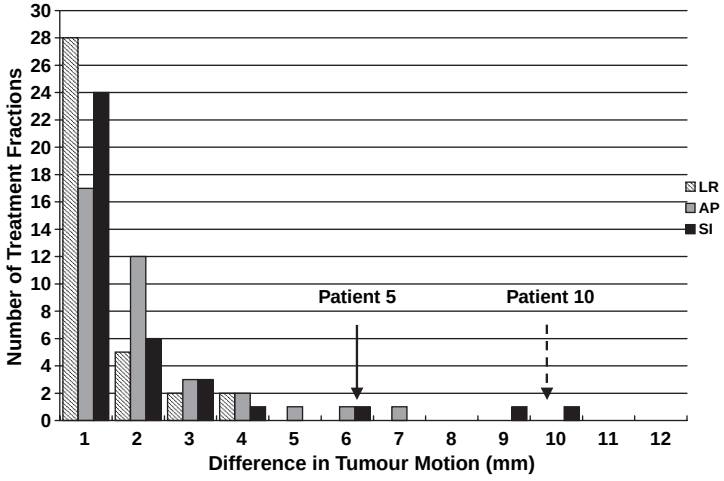

Figure 5. The difference in tumour motion between planning and treatment for 12 patients treated using SBRT. The results are consistent with the exception of two patients indicated by arrows.

These results suggest that the application of breathing motion data acquired at scanning time for gating radiation therapy treatment or real-time target tracking may not be suitable for all patients. In addition, gated techniques suffer from longer treatment times — which are typically greater than 45 min for patients treated under free breathing, and increase the likelihood of intra-fraction motion.

Several investigators have addressed tumour motion in lung SBRT using abdominal compression. Hof et al. [20] showed tumour motion with abdominal compression applied was 3.1 (1–6.7) mm in the LR direction, 2.6 (1–5.8) mm in the AP direction and 5.1 (2.5–10) mm in the SI direction, respectively. The authors noted that in seven of the 21 measurements, the movement in LR direction and AP direction was greater than the movement in the SI direction. This is consistent with the data in Table II, in which patient 5 demonstrated average tumour motion of 4.5 mm in the LR direction, 3.9 mm in the AP direction and 0.7 mm in the SI direction under abdominal compression.

These results follow the work of Negoro et al. [21] using a fused linear accelerator-CT scanner. In their study, tumour motion was significantly reduced from 12.3 (8–20) mm during free respiration to 7.0 (2–11) mm in the SI direction with abdominal compression applied. In the current study, abdominal compression was applied in cases where tumour motion exceeded 10 mm based on fluoroscopy, prior to CT simulation. In Table II, four patients were treated with compression, all of which showed tumour motion less than 10 mm for all directions at the time of planning. However, in the case of patient 10, the SI tumour motion exceeded 10 mm in three of the four treatment fractions with a mean tumour motion of 12.2 mm according to respiration correlated CBCT.

When target motion residual from abdominal compression is accounted for, the setup reproducibility of the SBF has been shown to be roughly 5–6 mm in the LR direction, 4–5 mm in the AP direction and 7–8 mm in the SI direction [22,23]. From our data, the tumour motion is smaller than the reproducibility of the SBF. Therefore with an in-room image-guidance approach, both target motion assessment and precise target localization can be achieved with immobilization limited to evacuated bags. In addition, patient 10 demonstrated differences in target motion greater than the setup reproducibility of the SBF.

Sharpe et al. [18] showed in a phantom study the geometric accuracy of the Synergy system. The location of an unambiguous object was measured by CBCT and MV portal imaging and the error between the measurements within two standard deviation was <0.5 mm in all directions. In addition, the targeting accuracy of the system was examined for shifts of ± 1.5 cm in all directions from isocentre using an unambiguous object as the target. The error within two standard deviations was <1.2 mm in all directions.

Respiration correlated CBCT datasets are acquired with a single full projection CBCT scan, therefore there is no additional acquisition time to generate multiple respiratory phase datasets. In addition, from our experience with CBCT image guidance, the process employed for 4D image guidance is more efficient on the treatment unit than using MV portal imaging for target localization and kV fluoroscopy for target and diaphragm motion, in part, because kV cone-beam CT images are easier to interpret than MV portal images. For this approach the imaging dose is negligible relative to the high biologically effective doses typical for SBRT

and the small number of treatment fractions required for delivery.

As CBCT becomes more mature, the image-guidance process will not only include target localization and assessment of target motion as presented here, but will involve on-line 4D image-guidance strategies and adaptive planning based on CBCT images rather CT simulation. The ability to capture both spatial and temporal information about the target and normal tissues of interest on the treatment unit will necessitate changes to make use of the efficiencies image-guidance promises.

We have presented an image-guided approach using CBCT for lung SBRT. In addition to using the full projection CBCT image datasets for target localization, the respiration correlated CBCT datasets acquired retrospectively were used to assess tumour motion on the treatment unit. The relative motion and position of the tumour at the time of treatment was found to be significantly different from that of the planning 4DCT scan in a subpopulation of patients. Therefore, application of breathing motion data acquired at scanning time to modulate or gate radiation therapy may not be suitable for all patients. Hypo-fractionated treatment techniques, such as SBRT, are particularly sensitive to both spatial and temporal localization, in which targeting errors involving either missing targets or treating normal tissue are often unrecoverable.

References

[1] Blomgren H, Lax I, Göranson H, Kraepelien T, Nilsson B, Näslund I, et al. Radiosurgery for tumors in the body: Clinical experience using a new method. J Radiosurgery 1998;1:63–74.

[2] Uematsu M, Shioda A, Tahara K, Fukui T, Yamamoto F, Tsumatori G, et al. Focal, high dose, and fractionated modified stereotactic radiation therapy for lung carcinoma patients: A preliminary experience. Cancer 1998;82:1062–70.

[3] Nakagawa K, Aoki Y, Tago M, Terahara A, Ohtomo K. Megavoltage CT-assisted stereotactic radiosurgery for thoracic tumors: Original research in the treatment of thoracic neoplasms. Int J Radiat Oncol Biol Phys 2000;48:449–57.

[4] Uematsu M, Shioda A, Suda A, Fukui T, Ozeki Y, Hama Y, et al. Computed tomography-guided frameless stereotactic radiotherapy for stage I non-small cell lung cancer: A 5-year experience. Int J Radiat Oncol Biol Phys 2001;51:666–70.

[5] Hof H, Herfarth KK, Munter M, Hoess A, Motsch J, Wannenmacher M, et al. Stereotactic single-dose radiotherapy of stage I non-small-cell lung cancer (NSCLC). Int J Radiat Oncol Biol Phys 2003;56:335–41.

[6] Wulf J, Hadinger U, Oppitz U, Thiele W, Flentje M. Impact of target reproducibility on tumor dose in stereotactic radiotherapy of targets in the lung and liver. Radiother Oncol 2003;66:141–50.

[7] Sibley GS, Jamieson TA, Marks LB, Anscher MS, Prosnitz LR. Radiotherapy alone for medically inoperable stage I non-small-cell lung cancer: The Duke experience. Int J Radiat Oncol Biol Phys 1998;40:149–54.

[8] Uematsu M, Shioda A, Suda A, Tahara K, Kojima T, Hama Y, et al. Intrafractional tumor position stability during computed tomography (CT)-guided frameless stereotactic radiation therapy for lung or liver cancers with a fusion of CT and linear accelerator (FOCAL) unit. Int J Radiat Oncol Biol Phys 2000;48:443–8.

[9] Kuriyama K, Onishi H, Sano N, Komiyama T, Aikawa Y, Tateda Y, et al. A new irradiation unit constructed of self-moving gantry-CT and linac. Int J Radiat Oncol Biol Phys 2003;55:428–35.

[10] Onishi H, Kuriyama K, Komiyama T, Tanaka S, Sano N, Aikawa Y, et al. A new irradiation system for lung cancer combining linear accelerator, computed tomography, patient self-breath-holding, and patient-directed beam-control without respiratory monitoring devices. Int J Radiat Oncol Biol Phys 2003;56:14–20.

[11] Hoisak JD, Sixel KE, Tirona R, Cheung PC, Pignol JP. Correlation of lung tumor motion with external surrogate indicators of respiration. Int J Radiat Oncol Biol Phys 2004;60:1298–306.

[12] Jaffray DA, Siewerdsen JH, Wong JW, Martinez AA. Flat-panel cone-beam computed tomography for image-guided radiation therapy. Int J Radiat Oncol Biol Phys 2002;53:1337–49.

[13] Moseley DJ, Keller H, Siewerdsen JH, Jaffray DA. Framework for respiration correlated cone-beam computed tomography. Med Phys 2004;31:1778.

[14] Sonke JJ, Zijp L, Remeijer P, van Herk M. Respiratory correlated cone beam CT. Med Phys 2005;32:1176–86.

[15] Purdie TG, Moseley DJ, Sharpe MB, Bissonnette J-P, Jaffray DA. Image-guided process for 4D lung stereotactic body radiation therapy. Med Phys 2005;32:2135.

[16] International Commission on Radiation Units and Measurements (ICRU). Report 62: Prescribing, recording and reporting photon beam therapy (Supplement to ICRU Report 50). Bethesda, MD: ICRU Publications; 1999.

[17] Mageras GS, Pevsner A, Yorke ED, Rosenzweig KE, Ford EC, Hertanto A, et al. Measurement of lung tumor motion using respiration-correlated CT. Int J Radiat Oncol Biol Phys 2004;60:933–41.

[18] Sharpe MB, Moseley DJ, Purdie TG, Islam M, Siewerdsen JH, Jaffray DA. The stability of mechanical calibration for a kV cone beam computed tomography system integrated with linear accelerator. Med Phys 2006;33:136–44.

[19] Underberg RW, Lagerwaard FJ, van Tinteren H, Cuijpers JP, Slotman BJ, Senan S. Time trends in target volumes for stage I non-small-cell lung cancer after stereotactic radiotherapy. Int J Radiat Oncol Biol Phys 2006;64:1221–8.

[20] Hof H, Herfarth KK, Munter M, Essig M, Wannenmacher M, Debus J. The use of the multislice CT for the determination of respiratory lung tumor movement in stereotactic single-dose irradiation. Strahlenther Onkol 2003;179:542–7.

[21] Negoro Y, Nagata Y, Aoki T, Mizowaki T, Araki N, Takayama K, et al. The effectiveness of an immobilization device in conformal radiotherapy for lung tumor: Reduction of respiratory tumor movement and evaluation of the daily setup accuracy. Int J Radiat Oncol Biol Phys 2001;50:889–98.

[22] Wulf J, Hadinger U, Oppitz U, Olshausen B, Flentje M. Stereotactic radiotherapy of extracranial targets: CT-simulation and accuracy of treatment in the stereotactic body frame. Radiother Oncol 2000;57:225–36.

[23] Lax I, Blomgren H, Larson D, Näslund I. Extracranial stereotactic radiosurgery of localized targets. J Radiosurgery 1998;1:135–48.